

JAERI - M
87-038

SCALING OF THERMONUCLEAR FUSION NEUTRON
YIELD ON DOUBLET III TOKAMAK

March 1987

Mitsushi ABE^{*1}, Masayuki NAGAMI, Toshio HIRAYAMA
Akihisa KAMEARI^{*2}, Akio KITSUNEZAKI,
Shigeru KONOSHIMA, Michiya SHIMADA, T. ANGEL^{*3}
F. Blau^{*3}, R. Chase^{*3} and E. Fairbanks^{*3}

JAERI-M レポートは、日本原子力研究所が不定期に公刊している研究報告書です。
入手の問合わせは、日本原子力研究所技術情報部情報資料課（〒319-11 茨城県那珂郡東海村）
あて、お申しこしてください。なお、このほかに財団法人原子力弘済会資料センター（〒319-11 茨城
県那珂郡東海村日本原子力研究所内）で複写による実費頒布をおこなっております。

JAERI-M reports are issued irregularly.
Inquiries about availability of the reports should be addressed to Information Division, Department
of Technical Information, Japan Atomic Energy Research Institute, Tokai-mura, Naka-gun,
Ibaraki-ken 319-11, Japan.

© Japan Atomic Energy Research Institute, 1987

編集兼発行 日本原子力研究所
印刷 山田軽印刷所

SCALING OF THERMONUCLEAR FUSION NEUTRON YIELD
ON DOUBLET III TOKAMAK

Mitsushi ABE*, Masayuki NAGAMI, Toshio HIRAYAMA,
Akihisa KAMEARI*2, Akio KITSUNEZAKI, Shigeru KONOSHIMA,
Michiya SHIMADA, T. Angel*3, F. Blau*3,
R. Chase*3 and E. Fairbanks*3

Department of Large Tokamak Research
Naka Fusion Research Establishment
Japan Atomic Energy Research Institute
Naka-machi, Naka-gun, Ibaraki-ken

(Received February 9, 1987)

Fusion neutron yield during hydrogen neutral beam injection into the deuterium plasmas was examined and compared with neoclassical model, using the Doublet III data obtained in 1983. This provided scalings of thermonuclear fusion neutron yield for discussion on ion energy transport in tokamak devices.

Experimental data showed that fusion neutron yield appeared to have a scaling of $F \propto P_{abs}^4 I_p^2 \bar{n}_e^{-2}$ in low-recycling divertor discharges (so called H-mode). The neoclassical theory for ion heat conduction satisfactorily described the scaling of fusion neutron yield. With neutral injection power of $P_{inj} = 4.6 \text{ MW}$, the Doublet III deuterium plasma yielded thermonuclear neutrons at the rate of $1.2 \times 10^{13} \text{ (n/s)}$ in low-recycling divertor discharge, which was equivalent to the D^+T^+ -plasma with a

This work was performed under a cooperative agreement between the Japan Atomic Energy Research Institute and the United States Department of Energy under DOE Contract No. SE-AT03-80sf11512.

* On leave from Hitachi, Ltd.

*2 On leave from Mitsubishi Atomic Power Industries Inc.

*3 GA Technologies Inc.

thermonuclear fusion power multiplication factor $Q = 7.8 \times 10^{-5}$ or beam driven T^+ -plasma with $Q = 8.6 \times 10^{-2}$. Limiter discharge yielded fewer neutrons.

Keywords: Doublet III, Neutral Beam Injection, Thermonuclear Fusion, Scaling, Energy Transport, Tokamak, Deuterium Plasma

ダブレットⅢにおける熱核融合反応中性子発生率の比例則

日本原子力研究所那珂研究所臨界プラズマ研究部

阿部 充志^{*}・永見 正幸・平山 俊雄・亀有 昭久^{*2}

狐崎 晶生・木島 滋・嶋田 道也・T. Angel^{*3}

F. Blau^{*3}・R. Chase^{*3}・E. Fairbanks^{*3}

(1987年2月9日受理)

中性粒子入射加熱中の核融合中性子の発生量をダブレットⅢの重水素プラズマで調べた。使用した実験値は1983年の加熱量4.6 MWまでのデータである。これにより核融合中性子発生量について比例則を得ると共にイオンのエネルギー輸送について議論するため新古典理論による予測値と比較した。

実験結果は核融合中性子の発生量 F が低粒子リサイクリングのダイバータ放電(所謂Hモード)では、 $F \propto P_{abs}^{0.4} I_p^2 \bar{n}_e^{-2}$ に、比例することを示す。これは新古典理論による予測とよく一致する。4.6 MWの入射加熱量で核融合中性子は 1.2×10^{13} (個/秒)の発生率に達した(Hモード)。50% T^+ - 50% D^+ のプラズマに換算すると、核融合出力増倍係数 Q は、熱核融合反応により $Q = 7.8 \times 10^{-5}$ であり、100% T^+ のプラズマに換算すると、中性粒子入射による高速重水素との核融合反応により $Q = 8.6 \times 10^{-2}$ である。リミタ放電では核融合中性子の発生量は少ない。

那珂研究所：〒311-02 茨城県那珂郡那珂町大字向山801-1

* 日立製作所㈱

*2 三菱原子力工業㈱

*3 G A社

Contents

1. Introduction	1
2. Experiment	2
2.1 Experimental equipment	2
2.2 Neutron detecting system	2
3. Numerical simulation of fusion neutron yield	5
4. Results	8
4.1 Experimental data	8
4.2 Dependence of F on T_e and P_{abs}	10
4.3 Dependence of fusion neutron yield on \bar{n}_e and I_p	12
4.4 Dependence of fusion output on the Lawson number $\bar{n}_e \tau_E$	14
4.5 Discussion	15
5. Conclusion	16
Acknowledgement	17
References	18

目 次

1. 緒 言	1
2. 実 験	2
2.1 実験装置	2
2.2 中性子検出器	2
3. 核融合中性子発生量の定量的検討法	5
4. 結 果	8
4.1 実験データ	8
4.2 核融合中性子発生量の電子温度と加熱量への依存性	10
4.3 核融合中性子発生量の電子密度とプラズマ電流への依存性	12
4.4 核融合出力のローソン数への依存性	14
4.5 討 論	15
5. 結 言	16
謝 辞	17
参考文献	18

1. Introduction

Energy confinement time τ_E or the Lawson number $n_e \tau_E$ is usually adopted as a parameter for performance of fusion devices. Even though the Lawson criterion may be satisfied with large n_e and τ_E , a fusion power output and fusion power multiplication factor would be a better parameters for a performance evaluation. An understanding of their scaling is necessary for the designing of reactors. In this paper we discuss scalings which govern fusion power output, on the basis of experimental data obtained from the Doublet III tokamak with neutral heating power up to 4.6MW, and we compare the scalings with results from neoclassical ion transport model.

A few papers have discussed the performance of experimental fusion devices from the view point of fusion output. Dawson et al.[1] proposed the production of fusion power with non-maxwellian ions due to neutral beam injection (i.e. beam-target fusion). To confirm this proposal, Strachen et al.[2] and Eubank et al.[3] carried out basic experiments with deuterium neutral beams and deuterium target plasmas. They showed that the energy distribution of non-maxwellian ions calculated by a classical slowing down model well described the experimental results for the fusion reaction.

About thermonuclear fusion with maxwellian ions, Pappas and Parker[4], and Grisham and Strachen[5], discussed scalings of fusion neutron yield of ohmically heated plasmas, but the plasma temperature was quite low in these plasmas compared with that of fusion reactors.

Recent tokamak research attained the improved energy confinement with diverted plasma during neutral beam injection (so called H-mode) [6]. The improved confinement was also obtained in Doublet III with plasma parameter of $T_i \simeq T_e \simeq 3\text{keV}$ and line density $\bar{n}_e = 7 \times 10^{13} \text{m}^{-3}$ at neutral beam injection of 4.6MW[7]. Neutron yield due to the $D(d,n)He^3$ fusion reactions reached $1.2 \times 10^{13} \text{(n/s)}$. Using those data we can examine scaling of fusion neutron yield at closer point of fusion reactor.

The purpose of this paper is to discuss the scaling laws of thermonuclear fusion neutron yield of neutral beam heated deuterium plasma(not beam-plasma reaction) and to make comparison with results of neoclassical model for ion energy transport. We used Doublet III data for these purposes, which were obtained in 1983 with neutral beam injection of up to 4.6MW[7].

2. Experiment

2.1 Experimental equipment

Doublet III was a medium size tokamak with the major radius of 1.41m and the minor radius of 0.42m[7,8]. H^0 -neutral beams were injected into deuterium plasmas at a nearly perpendicular angle of 27° on the magnetic axis. The neutral beams had an energy of 69-76keV. In this study the maximum injection power was 4.6MW.

Table I lists the diagnostic system used. A $2\omega_{ce}$ radiometer was employed to measure the electron temperature distribution which was calibrated by the center electron temperature $T_e(0)$ of the Thomson scattering. The electron density profile was deduced from the 4-channel line averaged densities obtained with CO_2 laser interferometers. Photo diode measures intensities of recycling light ($D\alpha/H\alpha$) from the plasma, which is proportional to the particle recycling rate in the plasma edge region. Although the major component of the signal was $D\alpha$ (main plasma) it included a small fraction of $H\alpha$ (from the neutral beams). The plasma cross sectional shape was calculated using MHD equilibrium code and magnetic data of 24 flux loops and 12 partial Rogowsky coils.

2.2 Neutron detecting system

Doublet III has three moderators for neutron measurements. Each moderator has 5 detectors of different sensitivities, changing working gasses, gas pressures, and sizes. Sensitivity varies between the detectors by a factor of 30. Since each detector has a range of

The purpose of this paper is to discuss the scaling laws of thermonuclear fusion neutron yield of neutral beam heated deuterium plasma(not beam-plasma reaction) and to make comparison with results of neoclassical model for ion energy transport. We used Doublet III data for these purposes, which were obtained in 1983 with neutral beam injection of up to 4.6MW[7].

2. Experiment

2.1 Experimental equipment

Doublet III was a medium size tokamak with the major radius of 1.41m and the minor radius of 0.42m[7,8]. H^0 -neutral beams were injected into deuterium plasmas at a nearly perpendicular angle of 27° on the magnetic axis. The neutral beams had an energy of 69-76keV. In this study the maximum injection power was 4.6MW.

Table I lists the diagnostic system used. A $2\omega_{ce}$ radiometer was employed to measure the electron temperature distribution which was calibrated by the center electron temperature $T_e(0)$ of the Thomson scattering. The electron density profile was deduced from the 4-channel line averaged densities obtained with CO_2 laser interferometers. Photo diode measures intensities of recycling light ($D\alpha/H\alpha$) from the plasma, which is proportional to the particle recycling rate in the plasma edge region. Although the major component of the signal was $D\alpha$ (main plasma) it included a small fraction of $H\alpha$ (from the neutral beams). The plasma cross sectional shape was calculated using MHD equilibrium code and magnetic data of 24 flux loops and 12 partial Rogowsky coils.

2.2 Neutron detecting system

Doublet III has three moderators for neutron measurements. Each moderator has 5 detectors of different sensitivities, changing working gasses, gas pressures, and sizes. Sensitivity varies between the detectors by a factor of 30. Since each detector has a range of

approximately 10^2 , the total range is 10^7 . The moderators have cylindrical shapes with a radius of 445mm and a height of 813mm. Detectors are placed at the center of the moderators. A 102mm thickness of paraffin which reduces the neutron energy is surrounding the detectors. Outside of the paraffine, a 0.76mm thick layer of cadmium strongly absorbs slow neutrons and 76.2mm thick layer of lead reduces any hard X-ray noise with no significant effect on the neutron signal. The resolution time is 10ms which is sufficiently short, relative to the energy confinement time 40-70ms of the plasma. This system has no capability for resolution of neutron energy.

One of the moderators is placed near the primary limiter and the others are placed on the other side of the tokamak. These placements ensure each moderator has different sensitivity ratios between photo neutrons produced locally at the primary limiter and fusion neutrons produced at the plasma axis uniformly in toroidal direction[9]. It is possible to subtract photo neutron yield from the total yield to get fusion yield, even in the condition in which photo neutron yield is equivalent with fusion neutron yield.

In order to measure neutron yield, calibration of (1) the detectors and (2) the effect of structures around the moderators should be done. For the calibration (1), a neutron source of Cf^{252} was placed near the moderator to examine the output of each detector. The ratio of detector 1-channel to the other detector counts inside the same moderator will give the relative calibration number. For the calibration (2), the neutron source was placed inside the Doublet III vacuum vessel to examine the output of each moderator under actual set-up conditions. The source was placed at the main limiter for the calibration of photo-neutrons and at several points on the plasma axis for the calibration of fusion neutrons. Since the fusion neutrons are mainly from the axis uniformly, it is possible to get sensitivity for fusion neutrons by averaging the sensitivity over the toroidal direction.

Measurement errors are possibly from random counting error and counting miss in high counting rate detectors. The former error source is estimated to be 10%, because the counting rate is around 100counts/10ms. The 2nd error is estimated to be less than 30% comparing with the next sensitivity detector. The total counting error is less than 40%.

It is possible to measure the neutron yield from rates of 1×10^8 to 5×10^{15} (n/s) using these three moderators.

3. Numerical simulation of fusion neutron yield

Simulation of fusion neutron yield were carried out using a one-dimensional transport code, in order to compare experimental neutron yield scalings with the results from neoclassical theory for ion heat conduction. The energy flow of ion channel across the minor radius r is described by the following equations [10,11,12]

$$\frac{\partial}{\partial r} (P_{bi} - P_{cd} - P_{cv} - P_{cx} - P_{ei}) = 0 \quad (1),$$

$$P_{cd} = -n_i A_r \chi_i \frac{\partial T_i}{\partial r}$$

$$P_{cv} = -\frac{5}{2} A_r T_i \Gamma_i$$

$$\chi_i = F_x \chi_i^{HH}$$

where P_{cx} , P_{ei} , P_{bi} are the integrated values of the charge exchange loss, the energy transferred from electrons and the energy transferred from neutral beams to ions respectively; T_i is the ion temperature; Γ_i is the particle flux of ions; χ_i^{HH} is the Hinton-Hazeltine's neoclassical heat conductivity[12]; F_x is an enhancement factor of neoclassical heat conductivity; A_r is a geometrical factor which reduces to the flux surface area, and r is a position in the minor radius direction.

P_{bi} is calculated by the Birth code[13]. P_{cx} , P_{ei} and Γ_i are calculated by the identical method as ref[10].

The input data of the simulation are electron density $n_e(r)$, electron temperature $T_e(r)$, and injected power P_{inj} . We assume the following equation for $n_e(r)$,

$$n_e(r) = n_e(0) (1.0 - (r/1.05a_p)^4) \quad (2).$$

This equation is consistent with the CO₂ interferometer measurement.

The electron temperature profile was taken from typical beam heated discharges for each plasma current I_p . Based on more than 100

shot data[7], the central electron temperature $T_e(0)$, in eV units, is taken as

$$\begin{aligned} T_e(0) &= 850 \times P_{abs} \text{ (MW)} && \text{(good confinement)} \\ T_e(0) &= (640 + 240 \times P_{abs} \text{ (MW)}) \times (\bar{n}_e / 5 \times 10^{19} \text{ m}^{-3})^{-0.5} && (3) \\ &&& \text{(poor confinement),} \end{aligned}$$

where \bar{n}_e is a line averaged electron density and P_{abs} is the power absorbed by a plasma from NB plus ohmic heating. The absorbed power from NB is defined from injection power P_{inj} subtracting the power of shine-through neutrals and ohmic power is $I_p V_l$, where V_l is the loop voltage.

The ion temperature is calculated with equation (1) using equation (1) and (2). The fusion neutron yield with maxwellian D^+ ions in plasma is calculated as

$$F_{th} = 0.5 \int_{V_p} n_D^2 \langle \sigma v \rangle_M dV \quad (4),$$

where $\int_{V_p} dV$ means a volume integral in the plasma region, n_D is deuteron density, $\langle \sigma v \rangle_M$ is the $D(d,n)He^3$ reaction cross section averaged over the velocity space with a maxwellian distribution at the ion temperature, and F_{th} is fusion neutron yield due to thermonuclear fusion. F_x of equation (1) is fixed at a certain value (usually 1.0, 4.0). Deuteron density n_D is determined by \bar{n}_e subtracting impurity and hydrogen fractions. The main impurity is assumed to be oxygen and its density was determined by $T_e(r)$ and loop voltage V_l through a assumption of uniform Z_{eff} . Hydrogen fraction is to be discussed later.

In the case of neutral beam injection (NBI) experiments, we have to pay some attention to the non-maxwellian distribution of high energy ions and fusion reaction due to them. Fusion neutron yield due to non-maxwellian ions is calculated by

$$F_b = \int_{V_p} \int_{1.5T_i}^{E_b} N_D(E) n_D \langle \sigma v \rangle_B dE dV \quad (5),$$

where $N_D(E)$ is density of high energy deuteron ion ($m^{-3}eV^{-1}$) at ion energy E , $\langle \sigma v \rangle_B$ is the $D(d,n)He^3$ reaction rate between high energy and thermal ions, and E_b is the energy of injected neutrals. The energy spectrum of $N_D(E)$ is obtained using the Fokker-Planck's slowing down model[14] and space distribution is calculated by the Birth code[13]. The origins of high energy deuteriums are contamination of the NB by D^0 , the natural isotope of hydrogen present in a 0.015% abundance, and collision of D^+ thermal particles with high energy H^+ (knock-on). Equation (5) was calculated, taking account of both high energy deuterium species. The results showed that F_b is less than 10% of F_{th} in Doublet III even in low temperature case ($1.0keV < T_i < 1.5keV$).

The fusion power multiplication factor Q is usually determined as $Q = P_f / P_{abs}$, where P_f is the power produced by nuclear fusion. We would like to define the following equivalent Q -values which are convenient for describing the situation of the Doublet III plasma in comparison with the reactor grade plasma.

- (1) Q_{th}^{50} : A fusion power multiplication factor of thermal fusion calculated by equation (4), with assumption of a 50% D^+ -50% T^+ plasma which has the same temperature and density as the Doublet III plasma.
- (2) Q_B^{100} : A fusion power multiplication factor including beam fusion calculated by equation (5), with assumption of deuterium neutral beams injected into 100% T^+ plasma which has the same temperature and density as the Doublet III plasma and assumption of ideal neutral beam of 90% 70keV(first species) neutral deuterium.

Besides the reaction for neutron production ($D(d,n)He^3$), there is another one ($D(d,p)T$). The sum of these two reaction is twice as large as the neutron yield. However in this research we considered only the neutron producing reaction and did not distinguish fusion neutron yield from fusion output.

Main error in calculating the fusion neutron yield comes from the uncertainty of hydrogen(H^0) contamination at plasma center region due to the NB and density profile[11]. We estimate the density fraction of

$H^0/(H^+ + D^+)$ at center region varying the particle confinement time τ_p (for H^+) from 10-30ms to 70-100ms depending on \bar{n}_e [11]. The estimated fraction is 10-30% at 4.6MW NB injection and the uncertainty of calculated fusion neutron yield is around 20%(high density)-50%(low density).

The calculating error due to the uncertainty of density profile was estimated by comparing the standard density profile as equation (2) and parabolic profile, which is equivalent with changing the ratio $n_e(0)/\bar{n}_e$ from ~ 1.05 to ~ 1.5 (standard $n_e(0)/\bar{n}_e$ of equation (2) is 1.2) [11]. This cause a uncertainty of 40% in calculated F .

The total calculating uncertainty is less than 60% at $P_{abs}/\bar{n}_e = 0.6$ (high density) - 1.5 (low density) ($\times 10^{-19} \text{ m}^3 \text{ MW}$), which is smaller than the raw data scattering of F in Doublet III experiments. This uncertainty is equivalent to $T_i(0)$ uncertainty of 20%, which is the same order uncertainty as PLT result of 20% with $P_{abs}/\bar{n}_e = 0.73$ ($\times 10^{-19} \text{ m}^3 \text{ MW}$) [2].

The estimation of Q_{th}^{50} has the same order uncertainty of 60%, and the uncertainty of Q_B^{100} , which has no dependence on density profile, is less than 50%

4. Results

4.1 Experimental data

We treated 180 neutral beam heated discharges. Table II gives the plasma parameters. H-mode plasma which has good confinements, appears on the divertor discharges with low particle recycling at edge plasma region (LR-divertor) [7].

Fig.1 shows time evolution of typical Doublet III discharges, comparing LR-divertor and limiter discharges at the same plasma current. Injection time length of NB is about 300ms which is much longer than the energy confinement time of up to 70ms. During the joule heating phase, neutron yield is 10^9 - 10^{10} (n/s). When the neutral beam injection starts, the neutron yield due to the thermonuclear reaction rises and reaches equilibrium value of 10^{11} - 10^{13} (n/s). Whereas in limiter

$H^0/(H^+ + D^+)$ at center region varying the particle confinement time τ_p (for H^+) from 10-30ms to 70-100ms depending on \bar{n}_e [11]. The estimated fraction is 10-30% at 4.6MW NB injection and the uncertainty of calculated fusion neutron yield is around 20%(high density)-50%(low density).

The calculating error due to the uncertainty of density profile was estimated by comparing the standard density profile as equation (2) and parabolic profile, which is equivalent with changing the ratio $n_e(0)/\bar{n}_e$ from ~ 1.05 to ~ 1.5 (standard $n_e(0)/\bar{n}_e$ of equation (2) is 1.2) [11]. This cause a uncertainty of 40% in calculated F .

The total calculating uncertainty is less than 60% at $P_{abs}/\bar{n}_e = 0.6$ (high density) - 1.5 (low density) ($\times 10^{-19} \text{ m}^3 \text{ MW}$), which is smaller than the raw data scattering of F in Doublet III experiments. This uncertainty is equivalent to $T_i(0)$ uncertainty of 20%, which is the same order uncertainty as PLT result of 20% with $P_{abs}/\bar{n}_e = 0.73$ ($\times 10^{-19} \text{ m}^3 \text{ MW}$) [2].

The estimation of Q_{th}^{50} has the same order uncertainty of 60%, and the uncertainty of Q_B^{100} , which has no dependence on density profile, is less than 50%

4. Results

4.1 Experimental data

We treated 180 neutral beam heated discharges. Table II gives the plasma parameters. H-mode plasma which has good confinements, appears on the divertor discharges with low particle recycling at edge plasma region (LR-divertor) [7].

Fig.1 shows time evolution of typical Doublet III discharges, comparing LR-divertor and limiter discharges at the same plasma current. Injection time length of NB is about 300ms which is much longer than the energy confinement time of up to 70ms. During the joule heating phase, neutron yield is 10^9 - 10^{10} (n/s). When the neutral beam injection starts, the neutron yield due to the thermonuclear reaction rises and reaches equilibrium value of 10^{11} - 10^{13} (n/s). Whereas in limiter

discharges the fusion neutron yield saturates early, in the LR-divertor discharges takes a long time for this to occur. This is because the energy confinement time is longer in the LR-divertor discharge and reached large neutron yield with long saturating time. The decay time of fusion neutron yield after neutral beam stopped, may have a information about the confinement time, however our discussion will be limited on the neutral beam heating phase, because we don't know whether the confinement properties in the decay phase is same as in the heating phase, or not. The data used in following discussion were sampled at 880ms in Fig.1 at which time the plasma is neutral beam heated and the neutron yield had attained its equilibrium value.

There are two kinds of neutrons, fusion neutrons and photo neutrons as mentioned in chapter 2. The latters are from the primary limiter[4,9]. In order to estimate their yields, we carried out experiments of hydrogen (H^+) plasma discharges with hydrogen (H^0) NB. The photo neutron reaction is the dominant neutron production process in these discharges. The neutron yield was less than 10^{10} (n/s) in the experiments. This results show that during neutral beam heating, photo neutrons are negligible compared with fusion neutrons in the NB heated deuterium plasma which has the neutron yield of 10^{11} - 10^{13} (n/s). We also obtained the same conclusion from the measurements with three moderators, which have the capability of distinguishing the two type of neutrons as described in Section 2.2. Ref.[7], which used the same data as this paper, showed that $T_e(0)$ is roughly same as $T_i(0)$ obtained from this neutron yield measurements. This fact also means that the measured neutrons are generated by the nuclear fusion.

Some parameters of LR-divertor plasma with 4.6MW injection are shown in Fig.2 which clarify the performance of Doublet III plasma. The spacial distribution of the fusion neutron yield F' (nm^{-3}/s) shows that almost all neutrons are from the inner area of $r \leq 0.5a_p$, and the fusion neutrons provide information on ion temperature T_i at the plasma center region, because the cross section of the $D(d,n)He^3$ reaction averaged by a maxwellian velocity distribution of T_i , is

strongly depends on T_i and roughly proportional to T_i^4 . Collision frequency ν^* deeply dropped into banana regime. Ion temperature was determined to fit the fusion neutron yield, changing the enhancement factor of neoclassical heat conductivity F_x to 5.3. T_i reached 2.7keV at center. The lowest plot shows the fusion power multiplication factor of equivalent D^+T^+ -plasma. At center region $Q_{th}^{50}=2 \times 10^{-3}$ or $Q_B^{100}=0.2$ and as a plasma volume average $Q_{th}^{50}=7.8 \times 10^{-4}$ or $Q_B^{100}=0.087$ are attained.

Energy transport analysis based on equation (1) showed that the main ion energy loss term at inner region area ($r < 0.8a_p$) is the conduction term $P_{cd} (= -n_i A_r \chi_i \partial T_i / \partial r)$. For example, the energy balance of discharge shown in Fig.2 at $r=0.5 a_p$ is $P_{bi}=710kW$, $P_{cd}=450kW$, $P_{ei}=-140kW$, $P_{cv}=160kW$ and $P_{cx}<10kW$. In the outer region P_{ei} term become the main energy flow term. At $r=0.8a_p$ P_{ei} is 510kW, while P_{cd} and P_{bi} are 420, 1130kW respectively.

Comparing these discharge characteristics with needs in the future fusion reactors, the density of $7 \times 10^{19} m^{-3}$ is almost the same, the ion temperature is 1/3 and the fusion power multiplication factor is 1/1000 of break-even condition for a thermal D^+T^+ -reactor and 1/10 of that for a beam-target fusion reactor.

4.2 Dependence of F on T_e and P_{abs}

A high electron temperature causes a large NB power to ions (P_{bi}) even \bar{n}_e , I_p and P_{abs} are kept constant. Experimental raw T_e data shows scattering of 20% in LR-divertor discharges[7]. This causes some uncertainty when we discuss the scaling law for fusion output. Fig.3 correlates T_e and F when P_{abs} , \bar{n}_e and B_T are kept constant. Experimental results for the operation condition $P_{abs}=3.7-4.3MW$ and $\bar{n}_e=5-7 \times 10^{19} m^{-3}$, are shown by the circles ($I_p=750kA$) and triangles ($I_p=480kA$). Open and shaded symbols denote H-mode and L-mode, respectively. Solid and dotted lines are simulation results using neoclassical ion heat conductivity at $I_p=750$ and $480kA$ for $\bar{n}_e=5.5 \times 10^{19} m^{-3}$, $P_{abs}=3.9MW$. The chained line is the ratio of the power

absorbed by ions (P_{bi}) to the injected power (P_{inj}).

Simulated results at $F_x=4.0$ are roughly consistent with the experimental ones. It becomes clear that $\pm 20\%$ variation of T_e in H-mode causes a $\pm 50\%$ variation in fusion output. This is the main reason of the raw data scattering of the fusion neutron yield and this variation is the same order as the calculating uncertainty discussed in chapter 3.

The L-mode has a large raw data scattering in T_e , which causes a large uncertainty in fusion neutron yield for the limiter discharges.

The discussion of the relation between T_e and F is only for estimation of the reason of raw data scattering. T_e depends strongly on heating power and we will take the heating power as a parameter of the discussion below.

Power dependence of the F-value is shown in Fig.4. Experimental results of fusion neutron yield at $\bar{n}_e = 5-6.5 \times 10^{19} \text{ m}^{-3}$, $B_T = 2.1-2.4 \text{ T}$ are shown by circles, triangles and squares which correspond to $I_p = 480, 600$ and 750 kA respectively. The open symbols denote divertor discharges with low particle recycling at the plasma edge (LR-divertor) and the shaded ones denote limiter discharges (L-mode). The two solid lines and one double chain line are the simulated results of equation (4), for LR-divertor and limiter discharges, respectively, at $F_x = 4, 8$, $I_p = 600 \text{ kA}$, $\bar{n}_e = 5.5 \times 10^{19} \text{ m}^{-3}$, and also 1/4 of the results with $F_x = 1$ are shown. The hatched area denotes the uncertainty of F due to the raw data scattering of $T_e(0)$ or the uncertainty of simulation of $F_x = 6.0$. The experimental results of the LR-divertor discharges are approximately proportional to P_{abs}^4 (chained line). The uncertainty in the simulated F is factor of 2.25, which mainly correspond to the raw data scattering of $T_e(0)$ and is smaller than factor of 2 change in F_x . F_x is estimated to be greater than 3 and less than 8 from Fig.4. This is consistent with ref.[7] and $F_x = 4.0$ is the reasonable value for the simulation of equation(1).

In limiter discharge, our simulation shows that F is proportional to P_{abs}^4 . However, the dependence of F on P_{abs} from experiment is not clear. The reason is supposed to be due to a large raw data scattering in $T_e(0)$.

The thermonuclear fusion rate $\langle \sigma v \rangle_M$ is proportional to T_i^{-1} ($l = 4.0 - 4.8$, $T_i = 1.5-3.0 \text{ keV}$). Then, $F \propto P_{abs}^4$ is equivalent with that $T_i(0)$ is roughly proportional to P_{abs} ($T_i(0) \propto P_{abs}^{1 \pm 0.2}$).

4.3 Dependence of fusion neutron yield on \bar{n}_e and I_p

Fig.5 shows the relation between normalized F and \bar{n}_e , I_p . Solid lines and dashed lines are simulated results of chapter 3, for LR-divertor and limiter discharge respectively, setting $F_x = 1.0, 4.0$. The results with $F_x = 1.0$ are divided by 4.

In Fig.5(a), F is normalized by P_{abs}^4 ($F^* = F/P_{abs}^4$). The

experimental data shows that the neutron yield decreases with increment of \bar{n}_e in both LR-divertor and limiter discharge when P_{abs} is kept constant. The simulated results have the same dependence as the experimental data and the dependence is as follows.

$$\begin{aligned} F/P_{abs}^4 &\propto \bar{n}_e^{-2} & (\text{LR-divertor}) \\ F/P_{abs}^4 &\propto \bar{n}_e^{-3} & (\text{limiter}) \end{aligned} \quad (6)$$

The experimental F has rather smaller value than the simulated value at $F_x=4$ in Fig.5(a), which suggest that F_x is roughly larger than 4. The reason why F decreases with \bar{n}_e is as follows.

Fusion reaction is proportional to \bar{n}_e^2 if T_i is kept constant. On the other hand, neoclassical heat conductivity χ_i^{HH} increases with \bar{n}_e . This cause a decrease of T_i . The D-D fusion reaction rate $\langle \sigma v \rangle_H$ has a dependence of approximately T_i^4 . Since the fusion reaction depends on both \bar{n}_e and T_i , the fusion neutron yield F decrease with \bar{n}_e . In the limiter discharge, F decreases rapidly with \bar{n}_e because T_e decreases with \bar{n}_e as given equation (3) and P_{bi} also decreases.

Fig.5(b) shows the I_p dependence of fusion neutron yield F which is normalized using the equation (6). Experimental data F are converted to normalised values at $\bar{n}_e = 5 \times 10^{19} \text{ m}^{-3}$ and $P_{abs} = 3 \text{ MW}$. The experimental data show that in both discharge modes, neutron yields are proportional to I_p^2 and the simulated results at $F_x=4$ also have the same dependence. The neoclassical heat conductivity χ_i has the dependence of I_p^{-1} when current profile is fixed. This cause a strong dependence of F on I_p . However, the I_p profile is peaked in low current discharges and the I_p dependence of F is modified to have the moderate dependence of I_p^2 .

In Fig.5(a) and (b), the simulated results with $F_x=1$ are shown as references. If we assume that $F_x=1$, the energy balance at $r=0.5a_p$ become changed to $P_{ei} \doteq P_{cd}$, where P_{cd} is the ion energy loss due to the neoclassical heat conduction ($P_{cd} = n_i \chi_i \partial T_i / \partial r$). P_{ei} has no dependence on I_p . This is why the fusion neutron has weaker dependence on I_p at $F_x=1.0$ than at $F_x=4.0$.

As fusion power output P_f is proportional to fusion neutron yield, we can define the fusion power multiplication factor Q' by

$$Q' = F / P_{abs} \quad (\text{ns}^{-1} \text{MW}^{-1}) \quad (7).$$

Power dependence of the factor Q' is shown in Fig.6. Q' was normalised by density into Q^* as

$$\begin{aligned} Q^* &= Q' / (\bar{n}_e / 5 \times 10^{19} \text{m}^{-3})^{-2} \\ Q^* &= Q' / (\bar{n}_e / 5 \times 10^{19} \text{m}^{-3})^{-3} \end{aligned} \quad (8).$$

Fig.6 shows that Q^* is proportional to $I_p^2 P_{abs}^3$ for the LR-divertor plasma and the scaling laws should be as follows,

$$\begin{aligned} Q^* &\propto I_p^2 P_{abs}^3 && (\text{LR-divertor}) \\ Q^* &\propto I_p^2 P_{abs}^{2.2} && (\text{limiter}) \end{aligned} \quad (9).$$

Scaling of fusion neutron yield or the fusion power is deduced from the equation (7), (8) and (9) as follows,

$$\begin{aligned} F^* &\propto P_{abs}^4 I_p^2 \bar{n}_e^{-2} && (\text{LR-divertor}) \\ F^* &\propto P_{abs}^{3.2} I_p^2 \bar{n}_e^{-3} && (\text{limiter}) \end{aligned} \quad (10).$$

The toroidal field strength B_T is not in the equation (10). The experimental data range is $B_T = 1.7\text{--}2.4\text{T}$ as Table II, and we have examined the B_T dependence of fusion yield. As a result we could not find the dependence and the fusion neutron yield has no dependence on B_T as far as our experimental data are concerned.

4.4 Dependence of fusion output on the Lawson number $\bar{n}_e \tau_E$

Since in the experimental fusion device, the injected power P_{inj} is limited rather than absorbed power P_{abs} , where $P_{inj} - P_{abs}$ is a shine-through of the neutral beam. In this sense, we will examine the fusion neutron yield at constant injection power. Fig.7(a) and (b) show the \bar{n}_e and $\bar{n}_e \tau_E$ dependence of F at constant injection NB power of $P_{inj} = 4.6\text{MW}$.

The \bar{n}_e dependence of the calculated result at $I_p = 480\text{kA}$ as well as experimental results are shown in Fig.7(a). Experimental results show that in LR-divertor discharge fusion neutron yield increases with increment of \bar{n}_e in low density region and in high density region the yield becomes saturated and decreases. In limiter discharges, the

yield F decreases monotonically with \bar{n}_e . These dependences are quite different from that of Fig.5(a), because in low density region the absorbed power strongly depends on \bar{n}_e and constant P_{inj} does not mean constant P_{abs} . The calculated results qualitatively explain the dependence and the saturation of neutron yield in high density region is due to the increase of neoclassical heat conduction.

The Lawson number $\bar{n}_e \tau_E$ is usually used as a parameter to show the performance of a fusion device. Fig.7(b) shows the relation between the fusion power multiplication factor Q' and the Lawson number $\bar{n}_e \tau_E$ at constant injection power of $P_{inj}=4.6\text{MW}$. When $\bar{n}_e \tau_E$ is less than $2.5 \times 10^{18} \text{m}^{-3} \text{sec}$, Q' increases with $\bar{n}_e \tau_E$, but when $\bar{n}_e \tau_E$ becomes larger than $2.5 \times 10^{19} \text{m}^{-3} \text{sec}$, Q' saturates. This is the same tendency as ref.[5]. The reason of this saturation is that high $\bar{n}_e \tau_E$ is attained by high density and increase of density saturates (or decrease) the fusion output as discussed on Fig.7. (a). The turn-over point is about the same as the PLT results of $\bar{n}_e \tau_{Ee} = 0.9 - 1.4 \times 10^{19} \text{m}^{-3} \text{sec}$, where $\bar{n}_e \tau_{Ee}$ is the electron Lawson number which under estimates the actual Lawson number by about a factor of two[5].

4.5 Discussion

The scaling of fusion neutron yield was found to be equation (10). However the gross energy confinement property[7] in thses data set is

$$\begin{aligned} \tau_E &\propto \bar{n}_e \\ \bar{n}_e \langle T \rangle &\propto \bar{n}_e P_{abs} \quad (\text{LR-divertor}) \end{aligned} \quad (11),$$

where $\langle T \rangle$ is a volume averaged temperature. The neutron yield should follows $F \propto n_e(0)^2 T_i(0)^4$, becuae $\langle \sigma v \rangle_M$ varies as roughly T_i^4 . If \bar{n}_e and $\langle T \rangle$ are proportional to $n_e(0)$ and $T_i(0)$ respectively, we get as a fusion yield scaling from equation (11),

$$\bar{n}_e^2 \langle T \rangle^4 \propto \bar{n}_e^2 P_{abs}^4 \quad (12).$$

This shows that scaling of neutron yield and the gross energy confinement is totally different. The fusion neutron yield depends on center ion parameter, but τ_E depends on the whole plasma parameters of all plasma region equally including electron parameters. Since the

energy flow mechanism is different between in ion and electron channel and also different between in edge and inner region of plasma, it is quite natural that equation (12) is different from equation (10).

Since main ion energy loss term in $r < 0.8a_p$ is conduction term P_{ed} and in $r > 0.8a_p$ it is the ion-electron rethermalization term P_{ei} , as mentioned in section 4.1, the central ion temperature is considered to be written as,

$$T_i(0) = a_p |\langle \nabla T_i \rangle| + T_i(a_p) \quad (13),$$

where the first term depends on the ion heat conduction and the second term is the edge ion temperature, and $\langle \nabla T_i \rangle$ is the average ion temperature gradient. From discussion of this paper it is reasonable that the first term of equation (13) has the neoclassical dependence. The second term $T_i(a_p)$ is controlled by the edge electron temperature, because the ion-electron rethermalization term is the main energy loss term in the edge plasma region. The low particle recycling gives the high electron temperature in the edge region[7] and the high edge electron temperature should give the high edge ion temperature in low recycling divertor discharges. It is reasonable to consider that this difference of the second term creates the difference of F between the LR-divertor and the limiter discharges.

5. Conclusion

Fusion neutron yield on Doublet III tokamak was examined, to get scaling of fusion power in tokamak devices. Experimental results were compared with the results calculated by a neoclassical model, with following results.

- (1) The fusion neutron yield F has a scaling of $F \propto P_{abs}^4 I_p^2 \bar{n}_e^{-2}$ for LR-divertor discharges and $F \propto P_{abs}^{3.2} I_p^2 \bar{n}_e^{-3}$ in limiter discharges, and fusion power output has the same scaling.
- (2) The neoclassical model of ion heat transport satisfactorily describes the scaling of fusion neutron yield in both LR-divertor and limiter discharges.
- (3) Plasmas in Doublet III are equivalent to the D^+T^+ plasma of

energy flow mechanism is different between in ion and electron channel and also different between in edge and inner region of plasma, it is quite natural that equation (12) is different from equation (10).

Since main ion energy loss term in $r < 0.8a_p$ is conduction term P_{ed} and in $r > 0.8a_p$ it is the ion-electron rethermalization term P_{ei} , as mentioned in section 4.1, the central ion temperature is considered to be written as,

$$T_i(0) = a_p |\langle \nabla T_i \rangle| + T_i(a_p) \quad (13),$$

where the first term depends on the ion heat conduction and the second term is the edge ion temperature, and $\langle \nabla T_i \rangle$ is the average ion temperature gradient. From discussion of this paper it is reasonable that the first term of equation (13) has the neoclassical dependence. The second term $T_i(a_p)$ is controlled by the edge electron temperature, because the ion-electron rethermalization term is the main energy loss term in the edge plasma region. The low particle recycling gives the high electron temperature in the edge region[7] and the high edge electron temperature should give the high edge ion temperature in low recycling divertor discharges. It is reasonable to consider that this difference of the second term creates the difference of F between the LR-divertor and the limiter discharges.

5. Conclusion

Fusion neutron yield on Doublet III tokamak was examined, to get scaling of fusion power in tokamak devices. Experimental results were compared with the results calculated by a neoclassical model, with following results.

- (1) The fusion neutron yield F has a scaling of $F \propto P_{abs}^4 I_p^2 \bar{n}_e^{-2}$ for LR-divertor discharges and $F \propto P_{abs}^{3.2} I_p^2 \bar{n}_e^{-3}$ in limiter discharges, and fusion power output has the same scaling.
- (2) The neoclassical model of ion heat transport satisfactorily describes the scaling of fusion neutron yield in both LR-divertor and limiter discharges.
- (3) Plasmas in Doublet III are equivalent to the D^+T^+ plasma of

fusion power multiplication factor $Q=7.8 \times 10^{-5}$ or T^+ plasma of $Q=8.6 \times 10^{-2}$ at the neutral beam injection power of 4.6MW.

The experimental results in this research are very encouraging, because increment of I_p and heating power results in a large increase of the fusion power multiplication factor.

Acknowledgement

The authors would like to thank Drs. S.Mori, Y.Iso, Y.Obata, K.Tomabechi, and M.Yoshikawa for their continuing encouragement throughout this work. The authors would also like to thank T. Ohkawa and the stuffs of GA Technologies Inc. for their continuing encouragement and valuable supports.

fusion power multiplication factor $Q=7.8 \times 10^{-5}$ or T^+ plasma of $Q=8.6 \times 10^{-2}$ at the neutral beam injection power of 4.6MW.

The experimental results in this research are very encouraging, because increment of I_p and heating power results in a large increase of the fusion power multiplication factor.

Acknowledgement

The authors would like to thank Drs. S.Mori, Y.Iso, Y.Obata, K.Tomabechi, and M.Yoshikawa for their continuing encouragement throughout this work. The authors would also like to thank T. Ohkawa and the stuffs of GA Technologies Inc. for their continuing encouragement and valuable supports.

References

- [1] DAWSON, J. M., FURTH, H. P., TENNEY, F. H., Phys. Rev. Lett. 26 (1977) 1156
- [2] STRACHEN, J. D., COLESTOCK, P. L., DAVIS, S. L., EAMES, D., EFTHIMION, P. C., et al. Nucl. Fusion 21 (1981) 67
- [3] EUBANK, H., GOLDSTON, R. J., ARUNASALAM, V., BITTER, M., BOL, K., et al. in Plasma Physics and Controlled Nuclear Fusion Research, 1978 (Proc. 7th int. Conf. Innsbruck, 1978) Vol.1 IAEA (1979) 167
- [4] PAPPAS, D. S. and PARKER, R. R. PFC/RP-78-5 MIT (1978)
- [5] GRISHAM, L. R. and STRACHEN, J. D. Nucl. Tech/Fusion 4 (1983) 46
- [6] WAGNER, F., BECKER, G., BEHRINGER, K., CAMPBELL, C., EBERHAGEN, A., et al. in Plasma Physics and Controlled Nuclear Fusion Research, 1982 (Proc. 9th Int. Conf. Baltimore, 1982) Vol.1 IAEA, Vienna (1983) 43.
- [7] NAGAMI, M., KASAI, M., KITSUNEZAKI, A., KOBAYASHI, T., KONOSHIMA, S., et al. Nucl. Fusion 24 (1984) 183
- [8] CALLERAINE, A. ARMENTROUT, C., BANDURRAGE, T., BEAL, J., BLAU, F., Heating in Toroidal Plasma (Proc. 3rd Joint Varenna-Grenoble Symposium 1982) Vol. 1 Euratom (1982) 49
- [9] PAPPAS, D. S., FURNSTAHL, R. J., KOCHANSKI, G. P., WYSOCKI, F. J., Nucl. Fusion 23 (1983) 1285
- [10] DÜCHES, D. F., POST, D. E., RUTHERFORD, P.H. Nucl. Fusion 17 (1977) 565
- [11] KASAI, M., NAGAMI, M., OTSUKA, M., AIKAWA, H., KITSUNEZAKI, A., et al., Nucl. Fusion 25 (1985) 1437
- [12] HINTON, F. L., and HAZELTINE, R. D., Rev. Mod. Phys. 48 (1976) 239
- [13] OTSUKA, M., NAGAMI, M., MATSUDA, T., Journal of Computational Physics 52 (1983) 219
- [14] SIVUKHIN V. D., Review Of Plasma Physics Vol. 4 (1966) 93 Consultant Bureau New York
- [15] YOKOMIZO, H., KONOSHIMA, S., AIKAWA, H., KASAI, M., NINOMIYA, H., et al. JJAP 21 (1984) 316

TABLE I DIAGNOSTIC SYSTEMS

Parameter	Diagnostic method
Center electron temperature	Thomson scattering
Electron temperature distribution	Electron cyclotron emission measurement at $2\omega_{ce}$
Center electron density	Thomson scattering
Line averaged density	4 channel CO ₂ laser interferometer
D α /H α intensity	Photo diode with filter

TABLE II PLASMA PARAMETERS IN THIS RESEARCH

Parameter	Value
Line averaged electron density \bar{n}_e	$2.5-7.5 \times 10^{19} \text{ m}^{-3}$
Plasma current I_p	0.35-0.75 MA
Neutral beam injection power P_{inj}	0-4.6 MW
Toroidal field B_T	1.7-2.4 T
Plasma shape	D(limiter), divertor

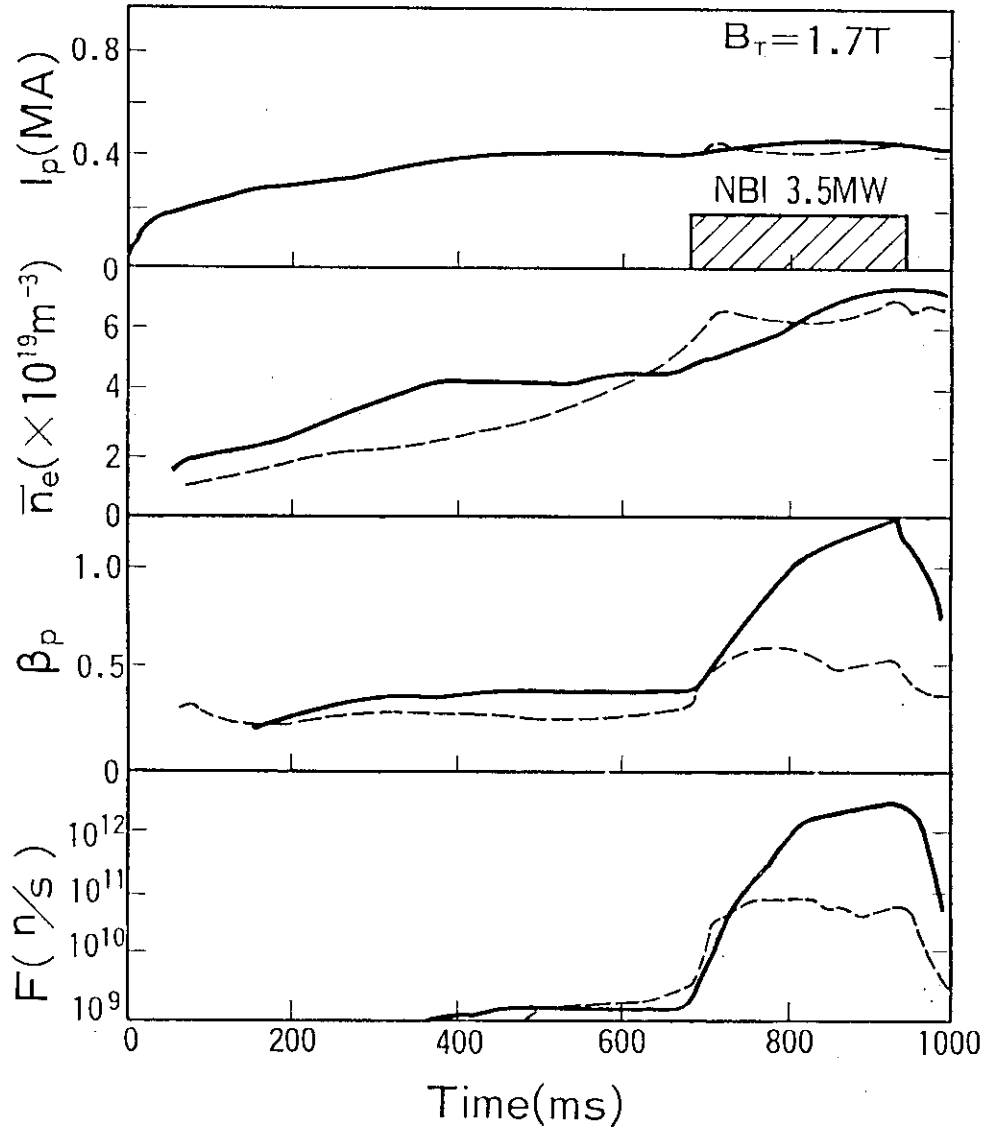


Fig.1 Time evolution of Doublet III discharge at $B_T=1.7T$.

Plasma current (I_p), line averaged electron density \bar{n}_e , poloidal beta value β_p and fusion neutron yield (F) are plotted. Solid line is a LR-divertor discharge (H-mode) and dashed line is a limiter discharge (L-mode). NBI is the neutral beam injection.

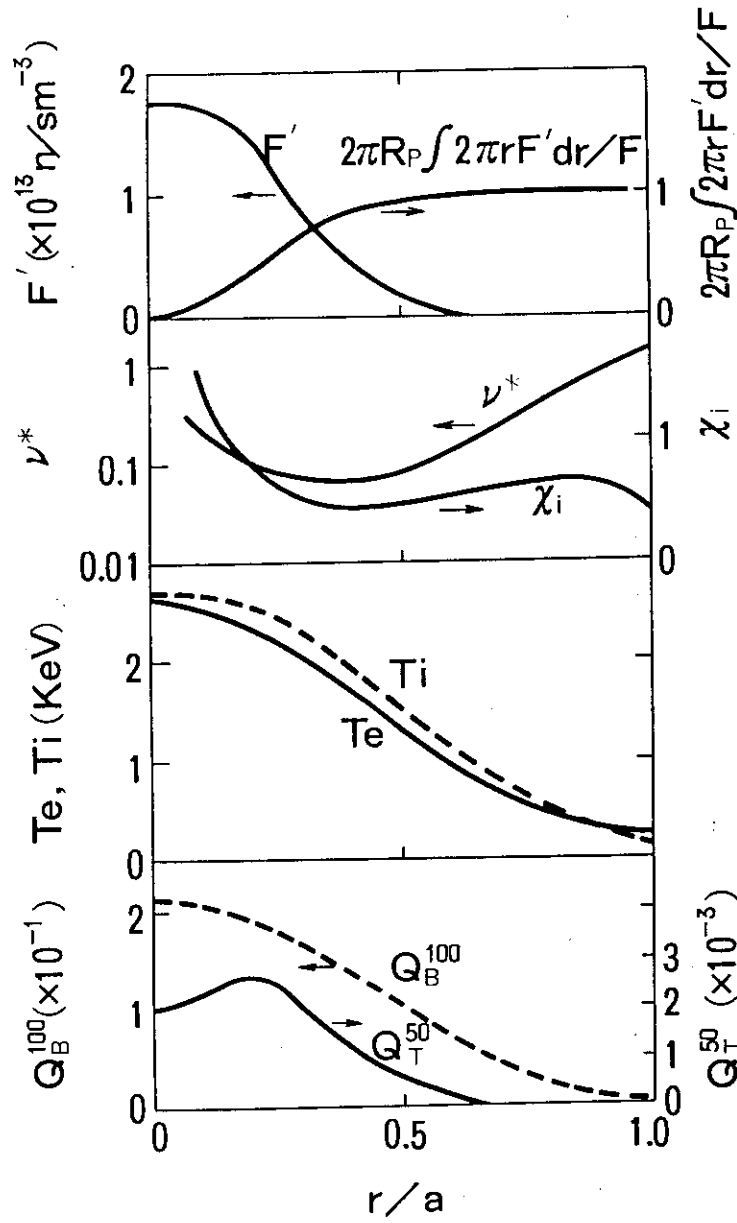


Fig.2 Distribution of parameters in low recycling divertor discharge (H-mode). Macro plasma parameters are $\bar{n}_e = 6.4 \times 10^{19} \text{ m}^{-3}$, $I_p = 750 \text{ kA}$ and $B_T = 2.1 \text{ T}$.

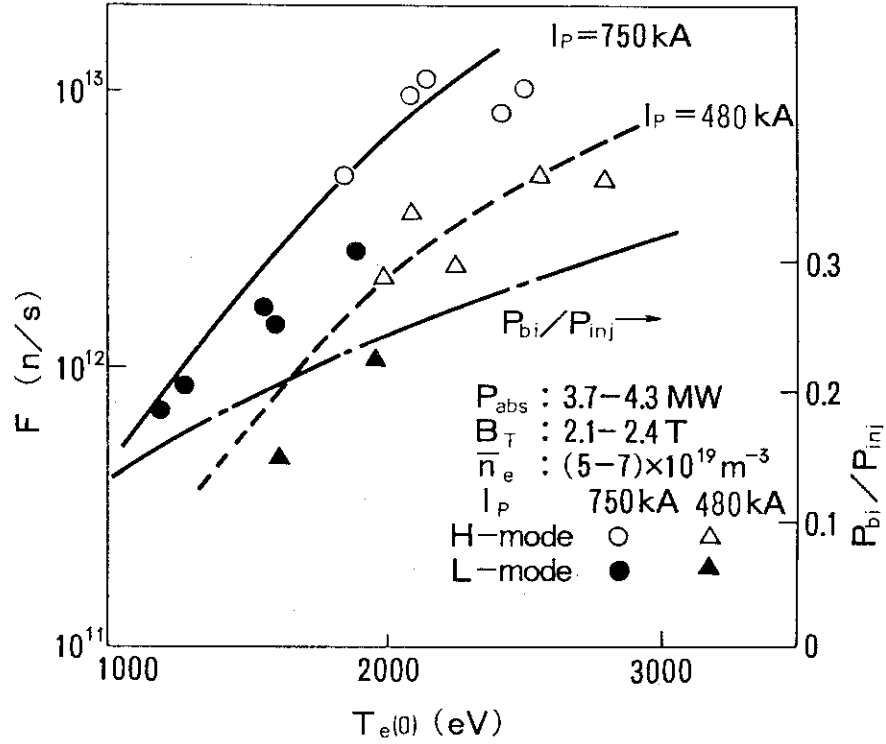


Fig.3 Center electron temperature vs. fusion neutron yield and heating power to ions with plasma current as a parameter.

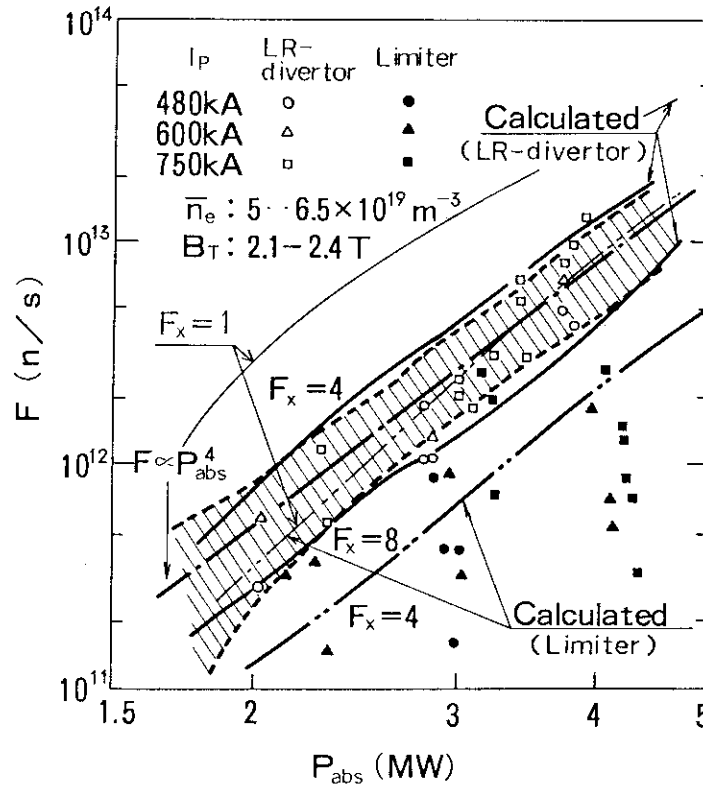


Fig.4 Absorbed power vs. fusion neutron yield. The hatched area denotes the calculation uncertainty due to raw data scattering of the center electron temperature. Calculation was carried out at $I_p=600\text{kA}$ and $F_x=8.0, 4.0, 1.0$.

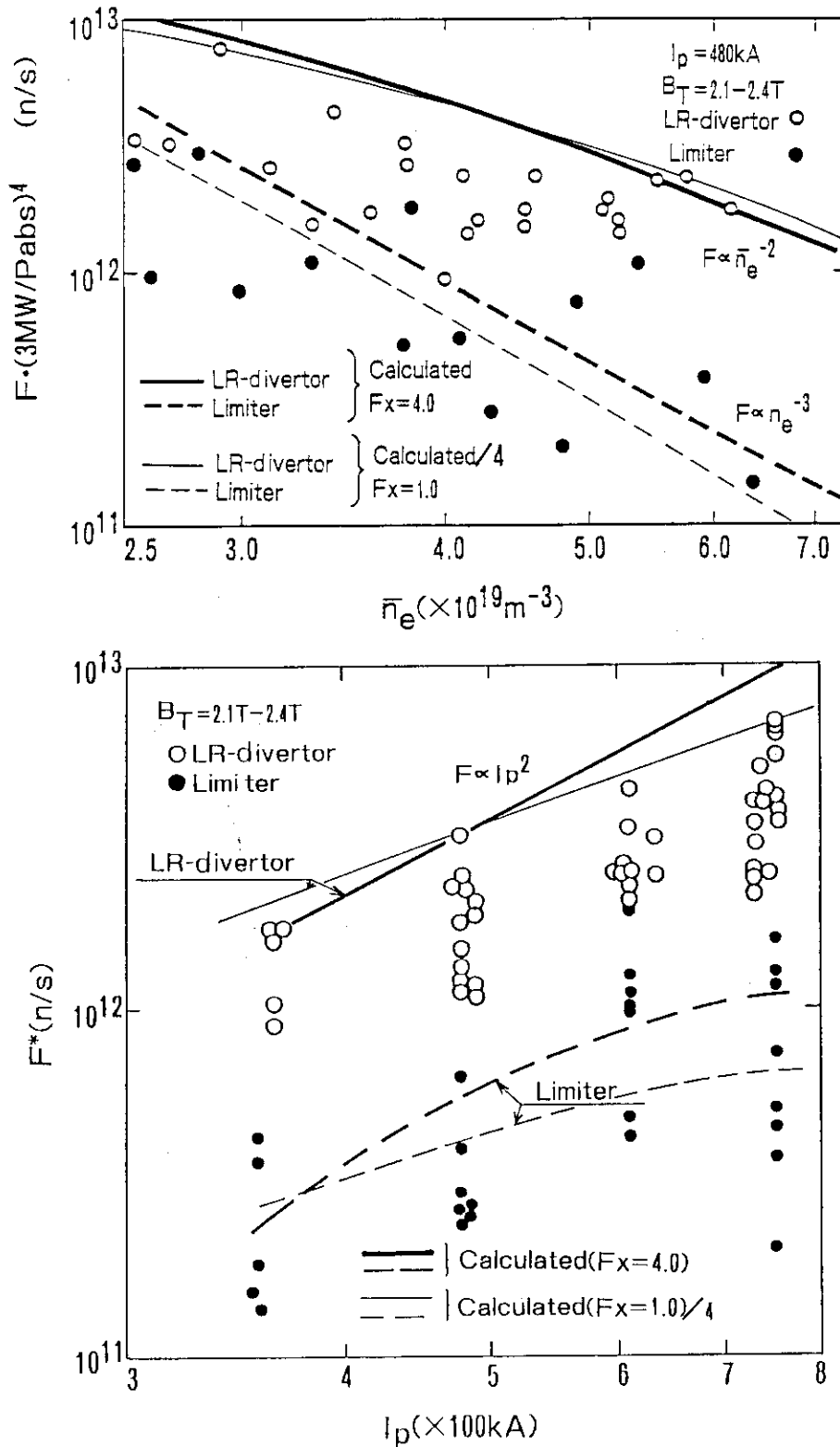


Fig. 5 Dependence of fusion neutron yield on \bar{n}_e and I_p , (a) \bar{n}_e dependence; (b) I_p dependence. F^* is the fusion neutron yield normalized by the following equations.

$$F^* = F \cdot (P_{\text{abs}}/3\text{MW})^{-4} \cdot (\bar{n}_e/5 \times 10^{19} \text{m}^{-3})^{-2} \quad (\text{LR-divertor})$$

$$F^* = F \cdot (P_{\text{abs}}/3\text{MW})^{-4} \cdot (\bar{n}_e/5 \times 10^{19} \text{m}^{-3})^{-3} \quad (\text{limiter})$$

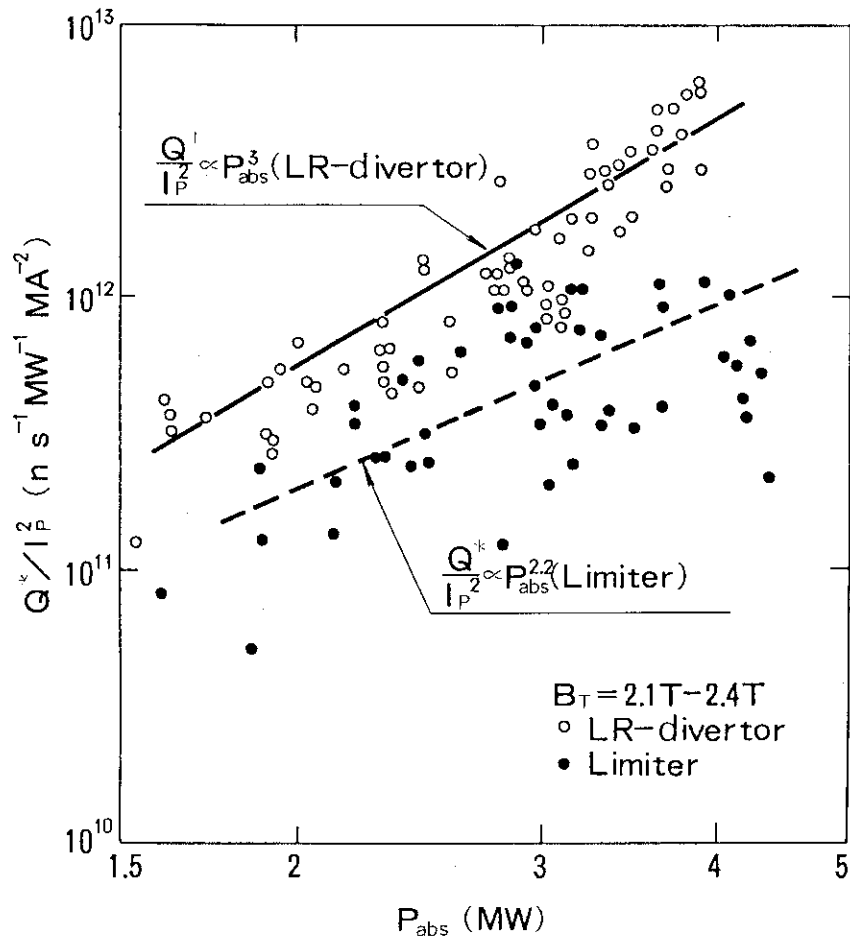


Fig.6 Scaling of the fusion power multiplication factor. Q^* is the normalized factor by \bar{n}_e using equation (8).

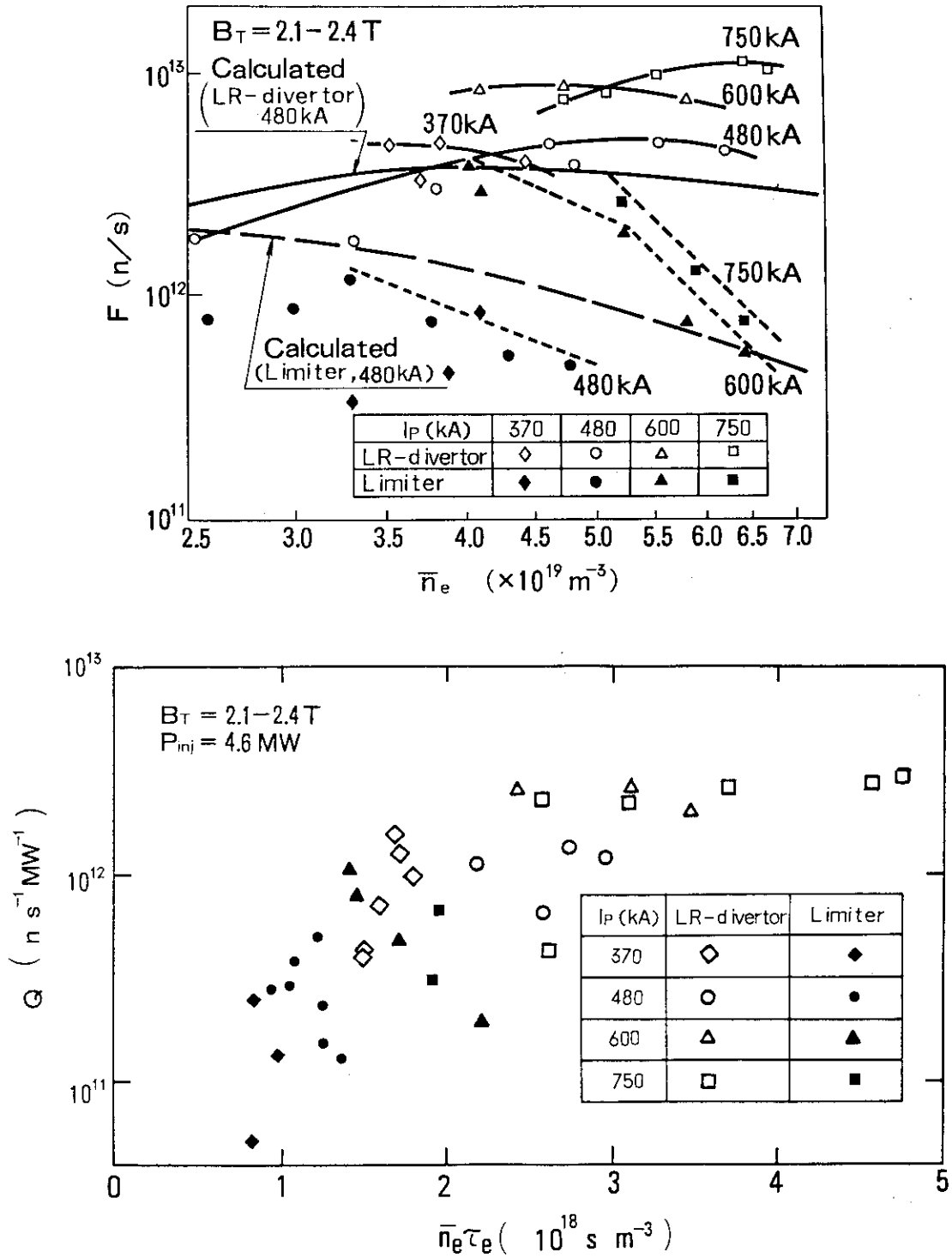


Fig.7 Dependence of fusion yield on \bar{n}_e and $\bar{n}_e \tau_E$ with constant injection power P_{inj} . (a) line averaged density vs. fusion neutron yield at constant P_{inj} ; (b) $\bar{n}_e \tau_E$ (the Lawson number) vs. fusion power multiplication factor Q . Fusion power saturate with high \bar{n}_e and $\bar{n}_e \tau_E$ value.